Article

Geochemistry of Chemical Weapon Breakdown Products on the Seafloor: 1,4-Thioxane in Seawater

Xin Zhang, Keith C. Hester, Oscar Mancillas, Edward T. Peltzer, Peter M. Walz, and Peter G. Brewer

Environ. Sci. Technol., **2009**, 43 (3), 610-615• DOI: 10.1021/es802283y • Publication Date (Web): 02 January 2009

Environ. Sci. Technol. **2009,** *43,* 610–615

Geochemistry of Chemical Weapon Breakdown Products on the Seafloor: 1,4-Thioxane in Seawater

XIN ZHANG,[†] KEITH C. HESTER,[‡] OSCAR MANCILLAS,[‡] EDWARD T. PELTZER,[‡] PETER M. WALZ,[‡] AND PETER G. BREWER*,[‡]

Key Laboratory of Ocean Remote Sensing of Ministry of Education of China, Ocean University of China, 5 Yushan Road, Qingdao 266003, P.R. China, and Monterey Bay Aquarium Research Institute, 7700 Sandholdt Road, Moss Landing, California 95039

Received August 14, 2008. Revised manuscript received November 7, 2008. Accepted November 13, 2008.

The long-term fate of chemical weapon debris disposed of in the ocean some 50 years ago, now sinking into marine sediments and leaking into the ocean environment, is poorly known. Direct evidence exists showing chemical weapon agents actively being released on the sea floor with detrimental effects including harm to marine life. Thus there is strong interest in determining the fate and lifetime of these materials, their decomposition products, and the affected zones around these sites. Here we study the geochemical properties of a mustard gas breakdown product, 1,4-thioxane (TO), using Raman spectroscopy. We show that TO forms a hydrate with a help-gas (a second guest added to stabilize the hydrate), such as methane or hydrogen sulfide, with the hydrate stability regime some 10 °C above pure methane hydrate. The temperature, pressure, and reducing conditions required for hydrate formation commonly occur at known disposal sites. The TO solubility was measured in seawater and found to vary from 0.65 to 0.63 mol/kg water between 4.5 and 25.0 °C. Similar to other hydrate systems, the TO solubility decreased in the presence of hydrate. A low solubility in water coupled with its ability to form a hydrate within marine sediments can greatly decrease molecular mobility and increase its lifetime. These results demonstrate how unanticipated reactions with marine sediments can occur, and how little is known of the processes controlling the environmental science of these materials.

Introduction

The Chemical Weapons Convention mandates the active destruction of chemical weapon (CW) stockpiles held by nations on land, but does not address the far larger quantities of "abandoned" CW that await passive environmental decomposition following disposal on the sea floor. At the end of World War II the warring nations had stockpiled large quantities of such material and this posed both an immediate and physically real danger, and a source of political concern. Convenient and rapid means of disposal were sought, and the ocean offered this opportunity. In the years immediately following World War II and until the signing of the London Convention in 1972, hundreds of thousands of tons of CW were disposed of in the Baltic and Adriatic Seas, off the east coast of Japan, in the Russian Arctic, and off the U.S. east and west coasts (*1, 2*). In many cases, the hasty means of disposal, poor record keeping, unauthorized activities (*3*), and the techniques of navigation at that time resulted in large uncertainties in location and depth, means of containment, and quantity of material disposed (*4*).

Some fifty years have now passed but still no national or international policies or programs exist to map and identify conditions at these sites (*5*). In the U.S., disposal was typically in deep water and far enough offshore that little contact with humans has occurred. But at sites closer to shore in the Baltic, and Adriatic, and off Japan, there have been some 500 cases of injury to fishermen over the decades since disposal took place (*4*). The rates of release are first due to corrosion of the containing casing, and then from decomposition of this material in seawater. Most reports suggest a 50 year time scale for the corrosion process, and we are now at about that point in time. Added to this is the evidence at many sites of battering of the casings by fishing gear, thus accelerating the release of CW agents. As an example, in a field site in the Adriatic, observations of agent spilling onto the sea floor, and subsequent harm to marine life. This was accompanied with the presence of TO directly measured in the surrounding sediment (*6*).

Mustard agent (1,1′-thiobis[2-chloroethane]) represents a large fraction of the disposed material and is thus a substance of significant concern; mustard itself is denser than seawater and will remain on the sea floor, forming a hard crust of hydrolysis products which slows decomposition. Mustard is hydrolyzed in seawater first to hemimustard, which then undergoes further hydrolysis to yield thiodiglycol and thioxane (TO, also known as 1,4-oxathiane) in a ratio of roughly 4:1 by the following overall reaction:

$$5\ \mathrm{Cl\text{-}C_2H_4\text{-}S\text{-}C_2H_4\text{-}Cl} + 9\ \mathrm{H_2O} \longrightarrow \quad (1)$$

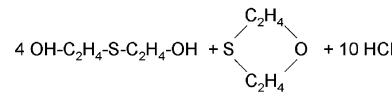

Mustard and its hydrolysis rate has been well studied in the laboratory (*7, 8*), but very little is known of the environmental complexities that may occur, such as within anoxic sediment pore waters. Knowledge of the decomposition pathways and the manner in which these CW agents interact with other oceanic geochemical processes is thus critical to predictions of the lifetime and fate of this material. Because of the hazards of the primary material, there is interest in estimating the contaminant halo in marine sediments and surrounding waters through detection and knowledge of the breakdown products. In this paper we examine the ocean geochemistry of TO as a critical indicator of the status of such sites and present new information on its solubility in seawater and its phase behavior in anoxic marine sediments.

Background. Our initial survey led us to realize that critical information on TO was missing; the solubility in seawater was not known and information on the interactions with marine sediments was completely lacking. Along with a higher density than seawater (1.114 g/mL at 25 °C versus 1.020−1.029 g/mL under typical ocean conditions), potential TO accumulation in these CW sites is strongly affected by its solubility. The reported TO solubility in water is limited to

* Corresponding author e-mail address: brpe@mbari.org.
[†] Ocean University of China.
[‡] Monterey Bay Aquarium Research Institute.

10.1021/es802283y CCC: $40.75
Published on Web 01/02/2009

a single value of 2.75 mol/kg H_2O (*2*) and the temperature dependence is not known.

In addition, the molecular size of TO suggested to us that it could form a solid clathrate hydrate in marine sediments (*9, 10*). There have been extensive studies on naturally occurring oceanic gas hydrates (*9, 11, 12*). Gas hydrates in nature are found to contain mostly methane from biogenic methanogenesis of organic carbon. However, mixed hydrate containing hydrogen sulfide have been observed under anaerobic conditions, often at sites of gas venting. Hydrates commonly occur in anoxic continental margin sediments including the Gulf of Mexico, the Blake Ridge, the Cascadia margin off the Pacific Northwest coast, offshore Japan, and in the Arctic. All of these areas are known to contain CW disposal sites (*11*−*13*). The marine geochemical behavior of a molecule trapped in a hydrate is strongly affected, slowing its transport and mobility in the surrounding sediments and shielding it from microbial degradation and further chemical attack while it is thus entrapped.

Experimental Section

Raman spectroscopy was chosen as the primary measurement tool because it permitted noninvasive investigation, thus minimizing laboratory hazards and simplifying high pressure measurements. TO possess a rich assortment of Raman-active modes available for measurement, and deep-ocean in situ Raman systems have now been developed thus potentially aligning the laboratory and field-investigative procedures (*14, 15*).

Laser Raman Spectrometer (LRS). A Kaiser Optical Systems, Inc. (KOSI) HoloSpec f/1.8i spectrometer (*16*) with a holographic grating and a front-illuminated cooled charge-coupled device (CCD) camera with 2048 × 512 pixels, by Andor Technology, was used in this study. The spectrum is split into two stripes on the face of the camera which maps to 1 Δcm^{-1} per pixel, measuring a spectral range from 100 to 4000 Δcm^{-1} with a resolution around 3 cm^{-1}. The Kaiser Mark II holographic stand-off optical probe (NCO-1.3-VIS), provided a ∼10× objective lens with a focal length in air of ∼6.4 cm. A frequency-doubled Nd:YAG laser (Coherent model DPSS532) operating at 532 nm, had a laser power of ∼28 mW (measured at the focal point of the optical probe). Spectra were acquired by KOSI's HoloGRAMS software, where dark spectrum subtraction and wavelength and intensity correction were performed during acquisition. Spectral analysis was performed using GRAMS/AI from Thermo Electron Corp.

Procedure. For measurement of TO in water under ambient pressure, various amounts of TO (Sigma-Aldrich, Inc., 98%) up to saturation, were added to pure water and seawater (Monterey Bay, CA) and agitated to facilitate mixing. The samples were placed in a jacketed glass container and temperature was controlled by circulating coolant water. The samples were allowed to equilibrate over 12 h at each temperature. To ensure equilibrium was achieved, multiple samples were intermittently measured over 72 h. In each case, before 12 h, the Raman intensity ratios were stable indicating that TO was no longer dissolving in the aqueous phase and it was assumed to have reached equilibrium. Multiple spectra were collected for each sample over a temperature range of 4−38.5 °C with a total acquisition time of 600 s per spectrum.

For measurements under pressure, TO and H_2O were combined in near equal amounts and agitated to facilitate mixing, resulting in two distinct liquid phases under ambient conditions. Around 4 wt% D_2O was added during the initial hydrate formation experiments to aid in structural identification. The aqueous solution, saturated in TO, was injected into a sapphire-windowed 1 cm^3 pressure cell, with a pressure range of 35 MPa, jacketed to allow for temperature control. An additional amount of pure TO was then injected to allow for changes in saturation conditions due to temperature, pressure, or hydrate formation. The system was pressurized with the desired gas and allowed to equilibrate. Hydrate formation was induced by cooling the system until nucleation was observed. Upon visual detection of a solid phase, Raman spectroscopy was used to interrogate all phases in the sample for each pressure condition. The system was then heated at around 1 °C per 10 min until the first observation of hydrate dissociation occurred to give an initial estimate of the dissociation temperature. At this point the system was cooled approximately 1.5−2 °C and temperature steps of 0.1 °C every 15 min, were used to determine the dissociation temperature. Hydrate dissociation was confirmed with both visual observation and Raman spectroscopic measurements (weakening and disappearance of the hydrate-related peaks). For a given pressure, multiple Raman spectra were collected for the aqueous sample with saturated TO, with both the presence and absence of the hydrate phase between 2.9−35.5 °C. The saturated sample was allowed to equilibrate over 12 h at each temperature. A total of 10 spectra were collected at each temperature with a total acquisition time of 600 s per spectrum.

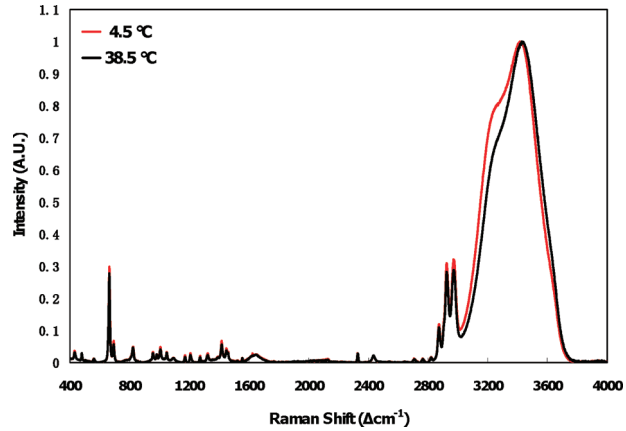

FIGURE 1. Raman spectra of 1,4-thioxane dissolved in seawater from 400 to 4000 Δcm^{-1} at 4.5 and 38.5 °C. The most intense vibrations from TO were two C−S stretching modes (ν_{15} 664 Δcm^{-1} and ν_{34} 693 Δcm^{-1}) and the CH_2 stretching modes (2850−3020 Δcm^{-1}) (*17*). Two seawater peaks, from the water bending (ν_2 ∼1640 Δcm^{-1}) and O−H stretching (3000−3800 Δcm^{-1}) modes, were also detected.

Results and Discussion

Raman Spectra of Aqueous TO Solutions. Raman spectra of TO dissolved in seawater at two different temperatures are shown in Figure 1. The strongest peaks from TO were from two C−S stretching modes (ν_{15}, 664 Δcm^{-1}, and ν_{34}, 693 Δcm^{-1}) and several CH_2 stretching modes (2850−3020 Δcm^{-1}) (*17*). The ν_{15} and ν_{34} modes for TO(aq) were found at approximately the same frequency as pure TO(l), whereas the TO(aq) peaks assigned to C−H stretching modes were blue-shifted between +15 and 18 Δcm^{-1} from TO(l).

Two peaks from water, the water bending mode (ν_2, ∼1640 Δcm^{-1}) and O−H stretching modes (3000−3800 Δcm^{-1}), were also present. The water O−H stretching peak, consisting of a complex profile of several vibrational modes, overlaps the TO−CH_2 stretching modes (*18*−*20*). A change of the shape of the water O−H stretching peak was also observed between 4.5 and 38.5 °C, which was attributed to decreased hydrogen bonding at higher temperatures (*20*). The ν_2 water bending mode was not convoluted with TO peaks and its shape showed little temperature dependence.

Raman Spectral Processing. Raman scattering intensity can be expressed as

$$R = IKP\sigma C \qquad (2)$$

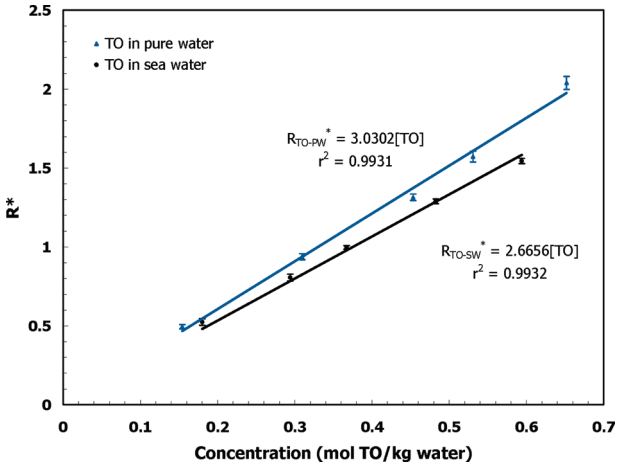

FIGURE 2. The normalized Raman peak area (R^*) versus TO concentration in pure water and seawater.

where R is the Raman peak intensity or area, I is the laser intensity, K accounts for instrument parameters including collection angle and efficiency, P is the optic path length of the sample, σ is the Raman scattering cross-section, and C is the concentration (*21*). Because of difficulties in quantifying I, K, and P, an internal reference standard is often required in order to obtain quantitative solubility data using Raman spectroscopy. To accomplish this, Raman peaks from the solute can be normalized with a peak from water. Due to its relative insensitivity to temperature and lack of overlapping peaks, the area of the two C−S stretching modes of TO were normalized with the ν_2 water bending mode (*22*). The normalized peak area has following relationship:

$$R^*_{TO} = \frac{R_{TO}}{R_{H_2O}} = \left(\frac{C_{TO}}{C_{H_2O}}\right)\left(\frac{\sigma_{TO}}{\sigma_{H_2O}}\right) \quad (3)$$

where R^*_{TO} is the normalized TO Raman peak area, R_{TO} is the integrated area of the TO ν_{15} and ν_{34} modes from 625 to 725 Δcm^{-1}, and R_{H_2O} is the integrated area of the water ν_2 mode from 1500 to 1800 Δcm^{-1}. Thus the normalized Raman peak area is directly proportional to the concentration ratio of TO and water (*22*−*24*).

Calibration of TO Concentrations from Raman Peak Intensities. Based on eq 3, the normalized TO peak area (R^*_{TO}) is a function of both the concentration and scattering cross section ratios of TO and water. It was assumed that the decrease in water concentration (due to dilution by TO) may be considered negligible when compared to the large observed increase in TO. However, the scattering cross section ratio is still unknown requiring a calibration curve to quantify TO concentration. This was performed by determining R^*_{TO} after adding known amounts of TO. If the scattering cross sections do not vary with TO concentration, from eq 3, it is expected that R^*_{TO} should be linearly correlated with TO concentration, similar to previous Raman studies with other solutes (*25*).

As shown in Figure 2, the experimentally determined calibration curve verified this linear behavior in both pure and seawater systems as given by the following relationships:

$$R^*_{TO-PW} = 3.0302[TO] \quad (r^2 = 0.9931) \quad (4)$$

$$R^*_{TO-SW} = 2.6656[TO] \quad (r^2 = 0.9932) \quad (5)$$

where R^*_{TO-PW} is the normalized Raman peak area for TO in pure water samples, R^*_{TO-SW} is the normalized Raman peak area for TO in seawater samples, and [TO] is the TO concentration in mol/kg H_2O. These correlations (eqs 4 and 5) were shown valid for four different temperatures (4.0, 4.5, 20.0, and 38.5 °C) in pure water and three different temperatures (4.5, 20.0, and 38.5 °C) in seawater indicating a negligible temperature effect of the Raman scattering cross section ratio. It is possible that the difference in R^* and the slopes of solubility versus temperature can be attributed to changes in the shape of the water peak (3000−3800 Δcm^{-1}) in pure water versus seawater systems.

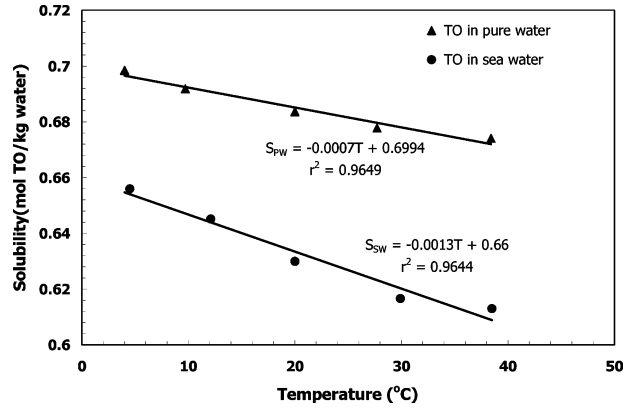

FIGURE 3. TO solubility with linear correlations both in the pure water and seawater systems between 4.0 and 38.5 °C.

TABLE 1. Five Measured Average Raman Normalized Peak Areas (R^*_{TO}) and Standard Deviation of TO Saturated Samples in Pure Water and Sea Water at Various Temperatures[a]

sample	temperature (°C)	average normalized peak area (R^*_{TO})	absolute average deviation (%)
TO in pure water	4.0	2.116	2.69
	9.7	2.096	2.39
	20.0	2.072	2.08
	27.7	2.054	2.78
	38.4	2.043	2.84
TO in seawater	4.5	1.749	2.86
	12.1	1.720	2.62
	20.0	1.679	3.87
	29.9	1.644	1.28
	38.5	1.634	2.20

[a] Note: 10 replicate measurements were averaged at each temperature.

TO Solubility in Sea Water. Employing the R^*_{TO} calibration curves (eqs 4 and 5), TO solubility in both pure and seawater was determined by measuring TO saturated aqueous solutions between 4.0 and 38.5 °C (Table 1). Figure 3 shows the relationship between TO solubility and temperature as given by

$$S_{PW}(mol/kgH_2O) = -0.0007T(°C) + 0.6994 \quad (r^2 = 0.9649) \quad (6)$$

$$S_{SW}(mol/kgH_2O) = -0.0013T(°C) + 0.6600 \quad (r^2 = 0.9644) \quad (7)$$

where S_{PW} is TO solubility in pure water and S_{SW} is TO solubility in seawater.

These results show that TO is only sparingly soluble in water, with a range of 0.63−0.65 mol/kg H_2O. It should be noted that the solubility determined in this study varies greatly from an earlier report of 2.75 mol/kg H_2O (*2*).

TO Hydrate Formation and Stability. Molecular size is the overwhelming criterion for hydrate formation (*25*). The estimated molecular diameter of TO was determined to be ~7 Å, similar to tetrahydrofuran and very close to the

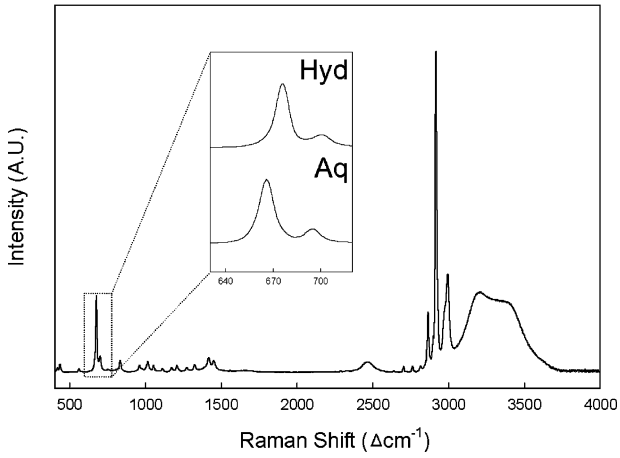

FIGURE 4. Raman spectrum of 1,4-thioxane + CH_4 hydrate from 400 to 4000 Δcm^{-1}. The peak at 2914 Δcm^{-1} was assigned to the ν_1 symmetric stretching mode of CH_4 in the 5^{12} cage. Other peaks present were assigned to TO and H_2O in the hydrate phase. The C−S stretching modes of TO exhibited the greatest shift upon enclathration. Insert shows the change in Raman shift for the ν_{15} and ν_{34} C−S stretching modes of TO in the hydrate (Hyd) phase versus the aqueous (Aq) phase (ν_{15}: +10 Δcm^{-1}, ν_{34}: +8 Δcm^{-1}).

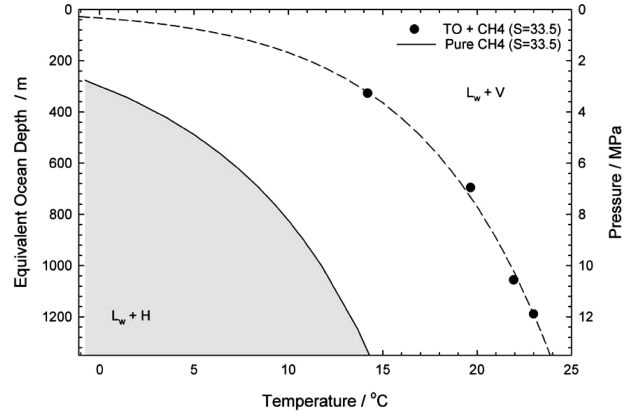

FIGURE 5. Temperature—Pressure (depth) equilibrium diagram showing the phase boundary for TO + CH_4 mixed hydrate (conducted in pure water and corrected for salinity) (*9*) and pure CH_4 hydrate formation with a salinity of 33.5. The dashed line is a fit to the experimental points. Adding TO results in a hydrate of greater stability (shift of over 10 °C). This implies that, with the exception of shallow sites such as the warm waters of the Adriatic and off Hawaii, almost all known ocean CW sites will fall within this phase space, including sites in the Baltic, the Arctic, Atlantic, and Pacific Oceans.

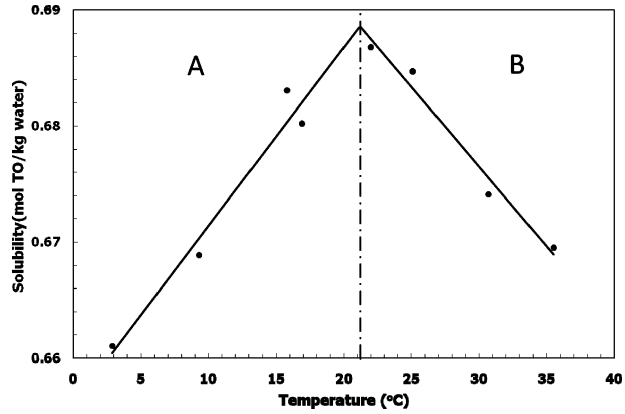

FIGURE 6. TO solubility from 2.9 to 35.5 °C at 8.85 MPa, both with presence (side A) and absence (side B) of hydrate. The TO solubility in water decreases with temperature in the presence of hydrate.

transition where a second guest is needed to stabilize the sII lattice. We therefore first examined whether TO alone would form a simple hydrate under ambient pressure, cooling to 273.25 K. After 48 h, hydrate formation was not observed under these ocean relevant temperature conditions. However, hydrate formation was quickly observed with the addition of the help-gas CH_4.

Raman spectroscopic measurements (Figure 4) confirmed the visually observed solid phase to be hydrate, with TO participating in the lattice. A peak at 2914 Δcm^{-1} was assigned to the ν_1 symmetric stretching mode of CH_4 in the 5^{12} cage (*26*). For TO, the largest change in Raman shift occurred for the C−S stretching modes. The ν_{15} (664 Δcm^{-1}) and ν_{34} (693 Δcm^{-1}) C−S stretching modes of TO dissolved in water remained unchanged from the pure liquid phase (*17*) but had a significant shift upon enclathration (ν_{15}: +10 Δcm^{-1}, ν_{34}: +8 Δcm^{-1}). For molecules entering the hydrate phase, this magnitude of frequency shift is routinely observed (*27*). Additionally, the isolated O−D stretching modes in the hydrate lattice (*28*) were Gaussian shaped, centered at 2545 Δcm^{-1} with a full width at half-maximum of 80 Δcm^{-1}. The visual presence of a solid and subsequent Raman evidence indicated a hydrate was formed. From both the size of TO and the O−D Raman stretching modes, the evidence supports sII as the lattice type. While we can qualitatively estimate the TO/methane ratio, quantitative information is not available for the hydrate guest concentrations using Raman spectroscopy.

To help generalize this result of TO hydrate formation, we replaced CH_4 by N_2 as the help-gas. Using a pressure of 15.8 MPa, formation of a TO + N_2 clathrate was readily observed upon cooling the system. Both the Raman shifts for TO and the isolated O−D modes of the water lattice were identical to those measured in the system with CH_4, indicating hydrate formation containing TO. This supports the idea that any guest molecule which stabilizes the 5^{12} cavity will form a mixed hydrate with TO under the appropriate conditions.

While the participation of TO in the hydrate was shown, the P−T stability must be determined to understand if hydrate formation could occur in known oceanic CW sites. Using a combination of visual and Raman measurements, the dissociation temperature of the mixed TO + CH_4 clathrate was determined in pure water over a range of relevant pressure conditions. Adding TO increased the overall hydrate stability versus the pure CH_4 hydrate by over 10 °C. While these experiments were performed in fresh water, a correction can readily be applied for saline ocean conditions (*9*). To determine where TO + CH_4 hydrate would be stable in comparison with known CW sites, we show in Figure 5 equilibrium stability curves for TO + CH_4 hydrate along with pure CH_4 hydrate. Almost all known CW sites, with the exception of the shallow warmer water sites (e.g., Hawaii, Adriatic), fall within the stability conditions for TO + CH_4 hydrate. A much more stable hydrate guest than CH_4 is H_2S, which will inevitably be present in any CH_4-rich sediment. While not measured in this study with TO, based on other studies of multicomponent hydrate systems, it can reasonably be inferred that any addition of H_2S will increase the overall hydrate stability (*9*) thus, further decreasing the depth at which binary hydrates with TO are stable and where the saturation conditions are met.

Anoxic conditions typically form within sediments under almost any structure placed on the sea floor (*29*),

and thus CH_4 and H_2S commonly occur at such debris sites covered in the various chemical weapon containers. TO has been found to accumulate in marine sediments and a saturated boundary layer should quickly form around the material within the sediment pore waters (*2*). Combined with low temperatures and high pressures at many of these debris sites, it is quite possible to have comingling of TO and CH_4/H_2S resulting in hydrate formation.

It should be noted that thiodiglycol is also formed during mustard hydrolysis, which would act as a hydrate inhibitor. However, thiodiglycol is highly soluble in seawater (56.5 mol/kg) and will be rapidly dispersed from a site; TO has a much lower solubility (Figure 3) resulting in a higher likelihood for accumulation in the sediments.

TO Solubility in the Presence of Hydrate. The solubility of TO in the presence of the (TO + CH_4) hydrate phase was measured between 2.9 and 35.5 °C at 8.85 MPa. As shown in Figure 6, the TO solubility in water decreases with temperature in the presence of hydrates in agreement with both theoretical and experimental results on other hydrate formers such as CH_4, liquid CO_2, and C_2H_6, where the solubility in water with presence and absence of the hydrate phase is well-known (*30*−*32*).

Ocean Geochemical Implications. The temperature, pressure, and reducing conditions required for hydrate formation commonly occur at known disposal sites. Similar to other hydrate systems 1,4-thioxane solubility decreased in the presence of hydrate; a lower solubility in water coupled with the ability to form a hydrate within marine sediments can greatly decrease molecular mobility and increase chemical lifetime.

The comingling of disposed weapons material with anoxic hydrate bearing sediments is not theoretical. As one practical example of this, the U.S. Ocean Drilling Program (ODP) in 1992 drilled site 889 on the Cascadia Margin to examine CH_4 hydrates (*33*). The operations report notes that "because the drill site was less than 10 m from the center of an old munitions dumping ground certain safety precautions were imposed by the Canadian government." These included a video survey of the sea floor, and a prohibition on coring the uppermost 20 m of sediment on the assumption that this was the maximum depth to which the munitions may have sunk in the mud. Yet another example is the Baltic Sea, where CH_4 gas has been shown to exist at shallow depths near a known CW site (*34*).

We have presented results for only one breakdown product of one CW agent; there are numerous such agents, including long-lived arsenical compounds with complex redox chemistry. Most environmental chemical predictions are based upon extrapolating oxic conditions and few direct measurements have been made to test these assumptions due to the obvious hazards of observation. The rapid development of in situ laser Raman spectrometry provides new opportunities for remote sensing of chemical processes in the ocean (*35*, *36*), and may provide an essential link between laboratory and field studies.

Acknowledgments

We acknowledge the support of the David and Lucile Packard Foundation through a grant to MBARI. X.Z. is supported by China Scholarship Council (CSC) study at MBARI; O.M. is supported by NASA Curriculum Improvement Grant through Hartnell College.

Literature Cited

(1) Mitretek Systems, Ocean dumping of chemical weapons. http://www.mitretek.org/home.nsf/homelandsecurity/OceanDumpChemWeap. 2004.

(2) Mitre Corp. *Ocean Dumping of Chemical Munitions: Environmental Effects in Arctic Seas*; MEDEA Report; Mitre Corp.: McLean, VA, 1997.

(3) Kurata, H. In *Chemical Weapons: Destruction and Conversion*; Stockholm International Peace Research Institute; Taylor and Francis: London, 1980; p 77−93.

(4) Brewer, P. G.; Nakayama, N. What lies beneath: A plea for complete information. *Environ. Sci. Technol.* **2008**, *42*, 1394–1399.

(5) Ember, L. R. Chemical arms treaty at 10. *Chem. Eng. News* **2007**, *85*, 23–26.

(6) Amato, E.; Alcaro, L.; Corsi, I.; Della Torre, C.; Farchi, C.; Focardi, S.; Marino, G.; Tursi, A. An integrated ecotoxicological approach to assess the effects of pollutants released by unexploded chemical ordnance dumped in the southern Adriatic (Mediterranean Sea). *Mar. Biol.* **2006**,

(7) Bartlett, P. D.; Swain, C. G. Kinetics of hydrolysis and diplacement reactions of β, β'-dichlorodiethyl sulfide (mustard gas) and of β-chloro-β-hydroxydiethyl sulfide (mustard chlorohydrin). *J. Am. Chem. Soc.* **1949**, *71*, 1406–1415.

(8) Yang, Y.-C.; Ward, J. R.; Wilson, R. B.; Burrows, W.; Winterle, J. S. On the activation energy for the hydrolysis of bis(2-chloroethyl) sulfide. II. *Thermochim. Acta* **1987**, *114*, 313 317.

(9) Sloan, E. D.; Koh, C. A. *Clathrate Hydrates of Natural Gases*, 3rd ed.; CRC Press-Taylor and Francis Group: Boca Raton, FL, 2007.

(10) Ripmeester, J. Hydrate research - from correlations to a knowledge-based discipline: The importance of structure. *Ann. N. Y. Acad. Sci.* **2000**, *912*, 1–16.

(11) Tréhu, A. M.; Ruppel, C.; Holland, M.; Dickens, G. R.; Torres, M. E.; Collett, T. S.; Goldberg, D.; Riedel, M.; Schultheiss, P. Gas hydrates in marine sediments: Lessons from scientific ocean drilling. *Oceanography* **2006**, *19* (4), 124–142.

(12) Buffett, B. A. Clathrate hydrates. *Annu. Rev. Earth Planet. Sci.* **2000**, *28*, 477–507.

(13) Paull, C. K.; Ussler III, W.; Peltzer, E. T.; Brewer, P.; Keaten, R.; Mitts, P.; Nealon, J.; Greinert, J.; Herguera, J. C.; Perez, E. Authigenic carbon entombed in methane-soaked sediments from the northeastern transform margin of the Guaymas Basin, Gulf of California. *Deep-Sea Research II* **2007**, *54*, 1240 1267.

(14) Hester, K. C.; Dunk, R. M.; White, S. N.; Brewer, P. G.; Peltzer, E. T.; Sloan, E. D. Gas hydrate measurements at hydrate ridge using raman spectroscopy. *Geochim. Cosmochim. Acta* **2007**, *71*, 2947–2959.

(15) Hester, K. C.; Dunk, R. M.; Walz, P. M.; Peltzer, E. T.; Sloan, E. D.; Brewer, P. G. Direct measurements of multi-component hydrates on the seafloor: pathways to growth. *Fluid Phase Equilib.* **2007**, *261* (1−2), 396–406.

(16) Owen, H.; Battery, D. E.; Pelletier, M. J.; Slater, J. New spectroscopic instrument based on volume holographic optical elements. *Proc. SPIE* **1998**, *2406*, 60.

(17) Ellestad, O. H.; Klaboe, P.; Hagen, G. The infrared and Raman spectra of 1,4-thioxan: Force constant calculations and vibrational assignments for 1,4-thioxan and 1,4-dithian. *Spectrochim. Acta* **1972**, *28A*, 137–147.

(18) Walrafen, G. E.; Hokmabadi, M. S.; Yang, W.-H. Raman isosbestic points from liquid water. *J. Chem. Phys.* **1986**, *85*, 6964 6969.

(19) Terpstra, P.; Combes, D.; Zwick, A. Effects of salts on dynamics of water: A Raman spectroscopy study. *J. Chem. Phys.* **1990**, *92*, 65–70.

(20) Walrafen, G. E.; Yang, W. H.; Chu, Y. C. *Raman Evidence for the Clathrate-Like Structure of Highly Super Cooled Water-Supercooled Liquids*; ACS Symposium Series 676; American Chemical Society: Washington, DC, 1997; pp 287308.

(21) *Analytical Applications of Raman Spectroscopy*; Pelletier, M. J., Ed.; Blackwell Science Ltd.: Oxford, 1999, 478 pp.

(22) Ianoul, A.; Coleman, T.; Asher, S. A. UV resonance Raman spectroscopic detection of nitrate and nitrate in wastewater treatment processes. *Anal. Chem.* **2002**, *74*, 1458–61.

(23) Dunk, R. M.; Peltzer, E. T.; Walz, P. M.; Brewer, P. G. Seeing a deep ocean CO_2 enrichment experiment in a new light: Laser raman detection of dissolved CO_2 in seawater. *Environ. Sci. Technol.* **2005**, *39*, 9630–9636.

(24) Lu, W. J.; Chou, I. M.; Burruss, R. C. Determination of methane concentrations in water in equilibrium with sI methane hydrate in the absence of a vapor phase by in situ Raman spectroscopy. *Geochim. Cosmochim. Acta* **2008**, *72*, 412 422.

(25) Ripmeester, J. Hydrate research—From correlations to a knowledge-based discipline: The importance of structure. *Ann. N.Y. Acad. Sci.* **2000**, *912*, 1–16.

(26) Sum, A. K.; Burruss, R. C.; Sloan, E. D. Measurement of clathrate hydrates via Raman spectroscopy. *J. Phys. Chem. B* **1997**, *101*, 7371–7377.
(27) Subramanian, S.; Sloan, E. D. Trends in vibrational frequencies of guests trapped in clathrate hydrate cages. *J. Phys. Chem. B* **2002**, *106*, 4348–4355.
(28) Fleyfel, F.; Devlin, J. P. FT-IR Spectra of 90 K films of simple, mixed, and double clathrate hydrates of trimethylene oxide, methyl chloride, carbon dioxide, tetrahydrofuran, and ethylene oxide containing decoupled D_2O. *J. Phys. Chem.* **1988**, *92* 631.
(29) Westerlund, S. F. G.; Anderson, L. G.; Hall, P. O. J.; Iverfeldt, A.; Rutgers, M. M.; Loeff, V. D.; Sundby, B. Benthic fluxes of cadmium, copper, nickel, zinc, and lead in the coastal environment. *Geochim. Cosmochim. Acta* **1986**, *50*, 1289.
(30) Zatsepina, O. Y.; Buffett, B. A. Phase equilibrium of gas hydrate: Implications for the formation of hydrate in the deep sea floor. *Geophys. Res. Lett.* **1997**, *24*, 1567–1570.
(31) Kimuro, H.; Kusayanagi, T.; Morishita, M. Basic experimental results of liquid CO_2 injection into the deep ocean. *IEEE Trans. Energy Convers.* **1994**, *9*, 732–735.
(32) Gaudette, J.; Servio, P. Measurement of dissolved propane in water in the presence of gas hydrate. *J. Chem. Eng. Data* **2007**, *52*, 1449–1451.
(33) Shipboard Scientific Party. Leg 146 Preliminary Report, http://www-odp.tamu.edu/publications/prelim/146PREL.PDF, ODP Preliminary Report 1993; p 46.
(34) Thie*β*en, O.; Schmidt, M.; Theilen, F.; Schmitt, M.; Klein, G. Methane formation and distribution of acoustic turbidity inorganic-rich surface sediments in the Arkona Basin, Baltic Sea. *Cont. Shelf Res.* **2006**, *26*, 2469.
(35) Brewer, P. G.; Malby, G.; Pasteris, J. D.; White, S. N.; Peltzer, E. T.; Wopenka, B.; Freeman, J.; Brown, M. O. Development of a laser Raman spectrometer for deep-ocean science. *Deep-Sea Res., Part I* **2004**, *51*, 739–753.
(36) Pasteris, J. D.; Wopenka, B.; Freeman, J. J.; Brewer, P. G.; White, S. N.; Peltzer, E. T.; Malby, G. Raman spectroscopy in the deep ocean: successes and challenges. *Appl. Spectrosc.* **2004**, *58*, 195A–208A.

ES802283Y